

---

## ELECTRON IMPACT IONIZATION AND EXCITATION OF URACIL MOLECULES

M.I. SUKHOVIYA, M.I. SHAFRANYOSH, M.M. CHAVARGA,  
I.I. SHAFRANYOSH

PACS 30.34.50 Lf  
©2012

Uzhgorod National University  
(54, Voloshin Str., Uzhgorod 88000, Ukraine; e-mail: *ivanshafr@gmail.com*)

---

The cross-sections of the formation of positive and negative ions of uracil, a nitrogenous base of nucleic acids, are obtained experimentally. The values for negative ions were shown to reach their maximum of  $5.0 \times 10^{-18} \text{ cm}^2$  at an energy of bombarding electrons of 1.1 eV. The magnitudes and the energy dependence were determined for the cross-section of formation of positive uracil ions in the electron energy interval from the formation threshold to 200 eV. The ionization cross-section peak of  $(1.0 \pm 0.1) \times 10^{-15} \text{ cm}^2$  was found at an energy of 95 eV. The luminescence spectrum for isolated uracil molecules consisting of about 20 spectral bands and lines emitted under the action of slow electrons was obtained in the wavelength range 200–500 nm. The uracil radiation spectrum was shown to be driven by the processes of molecular dissociative excitation, dissociative excitation with ionization, and excitation of electron levels in the initial molecule and the molecular ion. The biophysical consequences of the results obtained are discussed.

---

### 1. Introduction

Early studies of the interaction between slow monoenergetic electrons and molecules of nitrogenous bases of nucleic acids have been started by the authors of this work as long ago as in the 1980s [1]. In our subsequent experiments [2, 3], the new methodological developments concerning the formation of the gas phase of molecules without appreciable degradation of their structures were implemented. In particular, we obtained intense molecular beams. This allowed us to reveal that the electron impact stimulates various physical processes in biomolecules, such as excitation, ionization, dissociative excitation, and dissociative ionization. We also evaluated the probability for each processes to take place at various electron energies.

An experimental study of the processes of inelastic interactions between biomolecules and slow electrons is associated, first of all, with the importance of the problem of intracellular irradiation of biostructures with secondary electrons that are formed in quantity in a substance subjected to irradiation of various kinds. In this connection, the physical modeling of the cell ioniza-

tion processes under laboratory experimental conditions, when the monoenergeticity and the single-action of electrons on biostructures can be provided in a wide enough energy range, is challenging. Information on the physical structure of molecules is necessary to understand the role of primary physical processes in the maintenance of the biosystem functioning and the influence of various environmental factors on this process. Among those factors, a special attention is paid to natural and artificial radiations. Generally speaking, the interaction between high-energy radiation and living cells does not give rise directly to the degradation of biopolymeric molecules, in particular, to the rupture of covalent bonds in the primary structure of nucleic acids. This action is executed by secondary electrons that are formed in quantity ( $4 \times 10^4$  electrons per 1 MeV of an incident high-energy particle) in a biosubstance [4]. The majority of secondary electrons is low-energetic (slow), with the energy ranging from fractions to tens of electronvolts [4]. It is slow electrons that are assumed today to be responsible for the main part of destructive changes at the molecular level in biostructures. The most important targets at that are genetic DNA and RNA macromolecules.

In our previous researches [5–7], we analyzed the processes of ionization and excitation of the molecules of nucleic acid bases, cytosine and thymine, in the gas phase by slow electrons. The present research is devoted to uracil.

### 2. Experimental Installations and Methods of Research

#### 2.1. Ionization

The experiment is based on a technique with the use of the intersecting beams of electrons and molecules, which was successfully applied earlier [5]. A beam of uracil molecules (see Fig. 1) was obtained with the use of a thermal effusion source of the multichannel type and a set of collimating slits. The effusion source included the following components: a copper container with an uracil

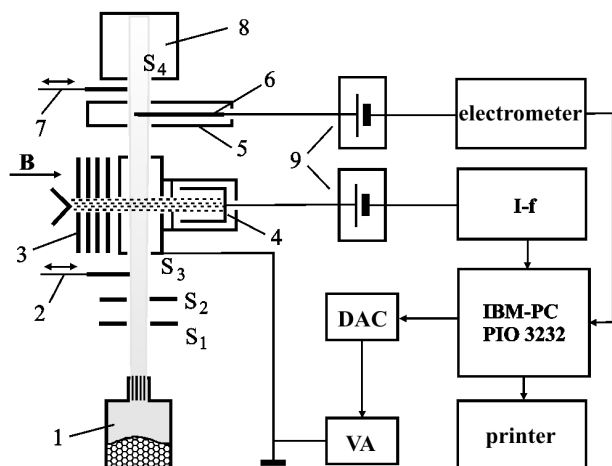


Fig. 1. Experimental setup for studying the ionization of uracil molecules: crucible (1), collimating slits (S1–S4), molecular beam latches (2 and 7), electron gun (3), electron collector (4), ion collector (5), probe (7), molecule collector (8), galvanic voltage sources (9), current-to-frequency converter (I–f), the digital-to-analog converter (DAC), and voltage amplifier (VA)

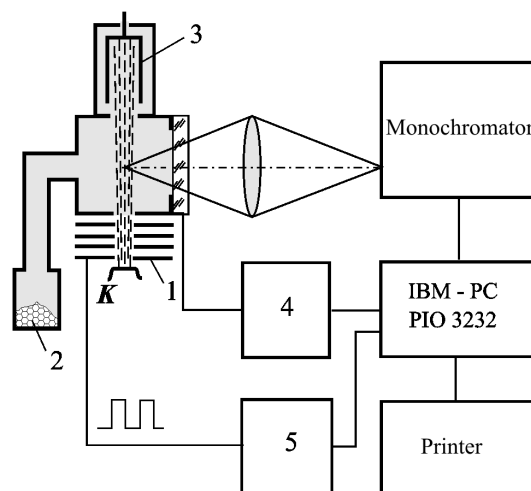


Fig. 2. Experimental setup for studying the excitation of uracil molecules: electron gun (1), electron emitter (K), uracil specimen (2), electron collector (Faraday cylinder) (3), source of the scanning potential of the electron beam (4), and block of modulation of the electron beam 5

specimen, the resistive heater of a container, a calibrated thermocouple (chromel–alumel) sensor of the temperature of a container, and thermal screens. The container itself was fabricated in the form of a hollow cylinder. An element with effusion channels (100 channels per an area of  $1.5 \times 1.5 \text{ mm}^2$ ) was mounted at one of the container ends and a hermetic choke at the other. The latter was used to arrange the uracil specimen with a purity of 99% (Sigma-Aldrich) and the temperature sensor. The heater was so designed that the temperature of an element with microchannels was by  $10 \text{ }^\circ\text{C}$  higher than that of the choke ( $93 \text{ }^\circ\text{C}$ ). In such a manner, we avoided the plugging of microchannels in the course of experiments. The molecules passed through the region of their interaction with the electron beam to be deposited at the end of their path onto the collector bottom and to form, in due course, an appreciable layer, the condensate. The collector comprised a cylindrical copper chamber with the input slit  $S_4$  and a flat bottom maintained at liquid nitrogen temperature. The measurements of the condensate mass and the time of its formation enabled us to determine the molecular beam intensity and, respectively, its concentration.

As a source of electrons, we used a five-electrode gun with a cathode made of thoriated tungsten. The electron gun temperature was kept constant at a level of  $110 \text{ }^\circ\text{C}$ , which provided the stability of parameters at the gun functioning. The first electrode of the gun was maintained at a low negative potential to filter out low-

energy electrons emitted from the cathode. The electrons in the beam that passed the collision region were captured by the Faraday cylinder that had a positive potential. The measurements were carried out at a current strength of  $1 \times 10^{-7} - 1 \times 10^{-6} \text{ A}$  in the electron beam and the half-height width of the electron energy distribution  $\Delta E_{1/2} \approx 0.3 \text{ eV}$ . The gun was arranged in a longitudinal field with the induction  $B = 1.2 \times 10^{-2} \text{ T}$ . The electron energy scale was calibrated according to the resonance peak of the formation of  $\text{SF}_6^-$  ions, the energy position of which was taken as the zero reference point.

To collect all ions that were formed in the region where the electron and molecular beams intersected each other, an intermediate collector with an axial electrode (a probe) was mounted at the molecular beam path. To provide the completeness of ion collection, the probe was maintained at a potential of  $25 \text{ V}$ , the polarity of which was determined by the charge sign of ions to be registered. The magnetic field prevented electrons that were scattered by uracil molecules and electrode surfaces from getting to the probe.

## 2.2. Excitation

The gas phase of uracil was formed by heating the specimen in a separate metallic container (Fig. 2). The obtained gas phase of uracil was directed by a steam line into a closed cubic mould (cell)  $2 \text{ cm}^3$  in volume. The temperature of the container with the uracil

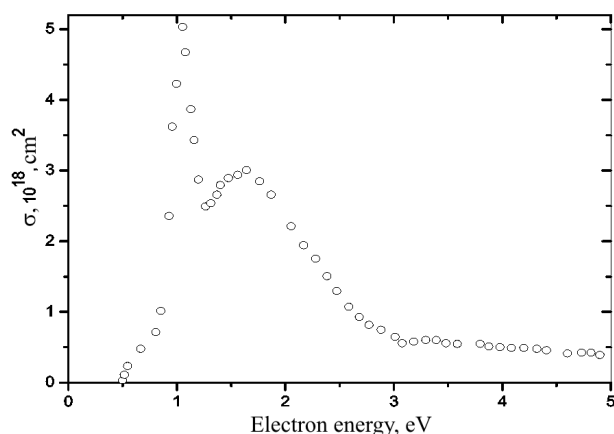


Fig. 3. Dependence of the cross-section of the formation of negative uracil ions on the electron energy

powder did not exceed 350 K. A diaphragm 1.5 mm in diameter for injecting the electron beam and the beam source itself were mounted on one of the external edges of the cell, and the electron beam detector (the Faraday cylinder) on the other. The electron beam was emitted by a five-electrode gun with a tungsten cathode. The cell was so embedded into a magnetic field that the electron beam propagated in parallel to the force lines of the field. The electron energy scale was calibrated with respect to the excitation threshold for the molecular nitrogen band at  $\lambda = 315.9$  nm (electron transition  $X^1\Sigma_g^+ - C^3\Pi_u$ , the second positive system) with an error of  $\pm 0.25$  eV. The magnetic field induction was about  $1.2 \times 10^{-2}$  T. For the radiation to leave the cell, a quartz window was mounted on its face. The radiation was registered with the use of a spectrophotometer consisting of a diffraction monochromator MDR-23 with a reverse dispersion of 1 nm/mm, a photoelectric multiplier FEU-106, and a system for the registration of photoelectric pulses. To improve the signal-to-noise ratio, the registration system was used in the photoelectric pulse counting mode, and the electron beam was modulated [5].

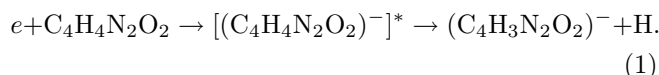
The experiments were carried out under the following conditions: the electron beam current strength fell within the limits  $(3 \div 4) \times 10^{-5}$  A, the half-height width of the electron energy distribution was  $\Delta E_{1/2} \approx 0.5$  eV, and the vacuum degree in the chamber where the cell with uracil vapors was arranged equaled about  $1 \times 10^{-5}$  Pa. To avoid the condensation of uracil vapors on the windows and the electrodes of an electron gun, the cell was heated up to a temperature of 370 K.

### 3. Research Results

#### 3.1. Ionization. Negative ions

In the course of our experiments, we found that negative ions of uracil are formed at the interaction of uracil molecules with the electron beam. For the first time, we experimentally measured the total effective cross-sections for the formation of negative uracil ions in the interval of electron energies from 0.4 to 5 eV. The results obtained are plotted in Fig. 3, where the energy of bombarding electrons is reckoned along the abscissa axis, and the ionization cross-section along the ordinate one.

It is evident from this figure that the formation of negative uracil ions has a resonance character with a maximum revealed at an electron energy of 1.1 eV. The magnitude of cross-section for the formation of negative uracil ions should be discussed separately. The maximum value of this parameter, according to our measurements, equals  $5 \times 10^{-18}$  cm<sup>2</sup>. The measured effective cross-section has the meaning of total cross-section, i.e. it includes the cross-sections corresponding to the formation of negative ions of both unbroken molecules and their fragments (the so-called partial cross-sections). However, according to the general physical ideas, if the concentration of interacting particles is low, the formation of an appreciable number of negative ions from unbroken molecules becomes almost impossible. Therefore, the generated negative ion of an unbroken molecule – following the conservation laws, it must be in an excited (electronic or vibrational) state – would most probably dissociate into a neutral and a charged fragment. In the low energy range of incident electrons – just this case is realized in our experiment – hydrogen atoms, which are characterized by the lowest binding energy with the pyrimidine ring [8], can be the most probable uncharged fragments. Therefore, the formation of negative ions will run in two stages,



Note that the estimation given in work [9] for the cross-section of negative uracil ion formation is by two orders of magnitude larger. However, in our researches, in contrast to work [9], we determined the concentration of molecules in the beam, with the other details of the routine being reliably approved [5]. Therefore, we consider the data of work [9] to be overestimated.

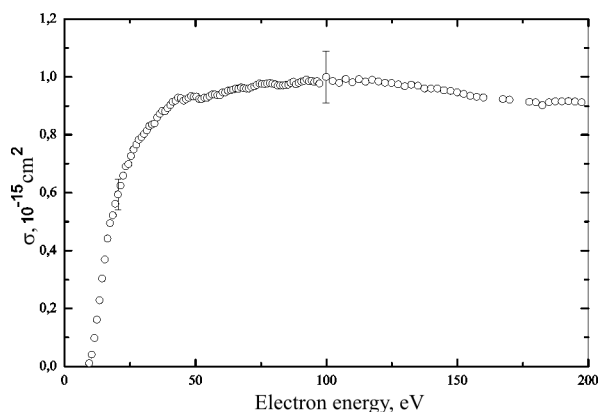


Fig. 4. Dependence of the total cross-section of the formation of positive uracil ions on the electron energy

### 3.2. Ionization. Positive ions

In the direct experiment, we determined the ionization cross-section and its energy dependence (the ionization function) for uracil in the energy interval of bombarding electrons from the threshold to 200 eV. The obtained data are plotted in Fig. 4. The figure demonstrates that, after the near-threshold growth, the ionization function of uracil molecules becomes rather flat, by revealing weakly pronounced features and a wide plateau. The maximum of the uracil ionization cross-section is located at an energy of 95 eV and equals  $(1.0 \pm 0.1) \times 10^{-15} \text{ cm}^2$ . The threshold of the formation of positive uracil ions was found to be  $9.4 \pm 0.2 \text{ eV}$ , which is in good agreement with the data obtained by other methods [10]. The cross-section of positive ion formation also has the meaning of total cross-section, i.e. it consists of the ion formation cross-sections for both initial molecules and their fragments (the partial cross-sections). A structure like a set of cusps is observed in the ionization curve. In our opinion, it stems from the contributions given by the formation of molecular ions in excited states and the dissociative ionization processes. The considerable cross-sections of dissociative ionization for the studied molecules (see below) give ground for this statement.

### 3.3. Mass spectra of uracil molecules

The results of mass-spectrometric studies (the fragmentary composition) of uracil obtained at an energy of bombarding electrons of 95 eV are exhibited in Fig. 5. The ratios  $m/z$  between the masses and the charges of ions measured in the system of atomic units are reckoned along the abscissa axis, and the intensities of the formed

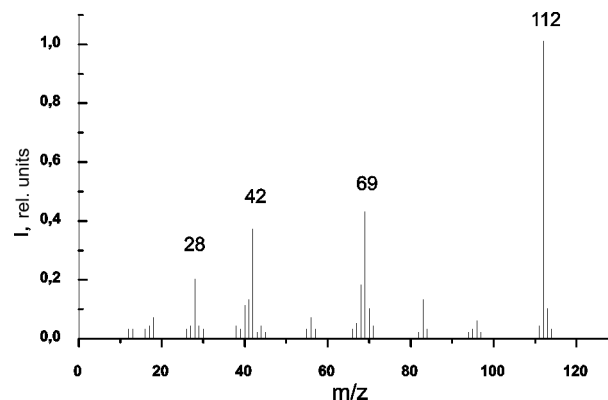


Fig. 5. Mass spectrum of uracil molecules

ions are reckoned in arbitrary units along the ordinate one. The characteristic features of the depicted mass spectrum include the presence of the most intensive line that corresponds to the single-charged molecular ion of uracil (the line at  $m/z = 112$ ), the presence of a considerable number of lines with different intensities that correspond to newly formed ionic fragments, and the absence of lines corresponding to double-charged molecular ions, as well as ions of di- and trimeric molecular compounds. The identification of lines in mass spectra was carried out by establishing their correspondence to the masses of probable fragments, making allowance for possible fragmentation scenarios. The known positions and regularities in the mass spectrometry of complicated molecules [11, 12] were taken into account at that.

A special attention should be paid to the comparison of mass spectra obtained by us with the results of other researchers. In Table 1, the relative intensities are presented for some mass spectral lines of uracil taken from various sources [13, 14]. It should be noted that the energies of bombarding electrons,  $E$ , at which the mass spectra were registered, were different a little. However, this circumstance does not substantially affect the relative intensities of the presented mass spectral lines, because the energy dependences of the partial ionization cross-sections are similar in the interval 75–120 eV [15].

From Table 1, it also follows that the results of our researches coincide with the results of work [13] to within the measurement errors, but differ from the data of work [14]. A possible explanation of this fact may consist in that the temperature of the working substance (used for obtaining the gas phase of uracil) was considerably different in our researches and in work [14]. Namely, it was equal to about 380 K in our research and in work [13], and to 423 K in work [14]. Whence a conclusion can be drawn that, starting from the temperatures of

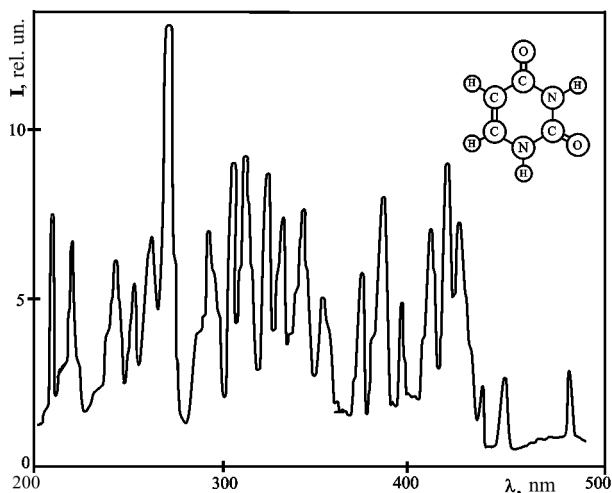


Fig. 6. Luminescence spectrum of uracil molecules at an electron energy of 100 eV

about 400 K, a substantial thermal fragmentation takes place in uracil molecules. In particular, a manifestation of this fragmentation is observed as a reduction of the relative intensities of mass spectral lines corresponding to molecular ions. Just this phenomenon is characteristic of the results of researches reported in work [14].

The data obtained for the total ionization cross-section of uracil molecules and their mass spectrum allowed us to determine the partial formation cross-sections for the ions of the most probable fragments of uracil molecules emerging at an energy of bombarding electrons of 95 eV (see Table 2). In Table 2,  $m/z$  means, in essence, the mass of molecular fragment in atomic mass units, and  $\sigma$  stands for the cross-section of the formation of the corresponding ionic molecular fragment.

It is pertinent to compare the cross-sections of the formation of positive ions, which were determined in our researches and in work [13]. From Table 3, it is evident that the corresponding values are different by a factor of

**Table 1. Relative intensities of uracil mass-spectral lines**

$m/z$	Ions	Intensity, rel. units		
		[14] $E = 75$ eV	[13] $E = 120$ eV	This work $E = 95$ eV
112	$C_4H_4N_2O_2^+$	1	1	1
69	$C_3H_3NO^+$	0.52	0.4	0.42
42	$CNO^+$ ; $C_2H_2O^+$ ; $CH_2N_2^+$	0.44	0.3	0.37
41	$CHN_2^+$ ; $C_2H_3N^+$	0.26	0.13	0.13
40	$C_2H_2N^+$ ; $CN_2^+$	0.28	0.11	0.11
28	$CO^+$	0.26	0.19	0.2

almost two. This discrepancy can be explained by the fact that the experimental results in work [13] were normalized to the results of theoretical calculations carried out in the framework of the semiclassical Deutsch–Mark formalism [16, 17], which is based on the Bethe approximation [18]. Therefore, Table 3 reflects, in essence, the level of consistency between our and theoretical data. It is well known [19] that the Bethe approximation overestimates the collision cross-sections in the low-energy interval.

### 3.4. Excitation

In this work, we experimentally measured the photoemission (luminescence) spectra of uracil in the wavelength interval 200–500 nm under the influence of the electron impact at various energies of bombarding electrons. In Fig. 6, the photoemission spectrum of uracil obtained at an electron energy of 100 eV is shown. The spectrum reveals pronounced molecular bands, the maxima of which are located at the wavelengths  $\lambda_M = 205.5, 218.5, 241.9, 254.0, 265.3, 277.4, 297.2, 310.0, 317.1, 328.4, 333.5, 344.5, 357.3, 377.1, 387.9, 398.0, 412.3, 421.0, 427.3, 451.1,$  and 486.1 nm. It is evident from the figure that almost all the bands have a complicated character, which testifies to their superposition origin. For the sake of comparison, we should notice here that the photoexcitation of polycrystalline uracil films produces a luminescence spectrum consisting of a wide smooth band in the wavelength interval between about 300 and 550 nm [20, 21].

It is rather difficult to correctly identify spectral bands with the use of the database available in the literature. However, despite of that, we succeeded in carrying out

**Table 2. Cross-sections of the formation of positive ions of uracil molecules and their fragments at an electron energy of 95 eV**

$m/z$	Ions	$\sigma, 10^{-16} \text{ cm}^2$
112	$C_4H_4N_2O_2^+$	2.69
96	$C_4H_4N_2O^+$	0.14
83	$C_3H_3N_2O^+$	0.34
70	$C_3H_4NO^+$	0.28
69	$C_3H_3NO^+$	1.14
68	$C_3H_2NO^+$ ; $C_4H_4O^+$	0.59
56	$C_2H_2NO^+$ ; $C_3H_4O^+$	0.18
42	$CNO^+$ ; $C_2H_2O^+$ ; $CH_2N_2^+$	0.99
41	$CHN_2^+$ ; $C_2H_3N^+$	0.34
40	$C_2H_2N^+$ ; $N_2^+$	0.30
28	$CO^+$	0.53
18	$H_2O^+$	0.20

the following analysis concerning the origin of bands in the spectrum obtained. For this purpose, we used the results of mass-spectrometric studies of uracil reported above and the data concerning the effective cross-sections for the total and dissociative ionization of uracil by the electron impact. In addition, we analyzed the photoemission spectra of relevant chemical compounds [21–25]. We also calculated the levels of electron excitation for the uracil molecule.

The data in Table 3 testify to a high probability of the uracil molecule fragmentation under the action of the electron impact. Of course, some of charged fragments are in excited states. In this case, it is necessary to pay attention, first of all, to those fragments, the partial formation cross-sections of which are the largest. These are the molecular ion  $C_4H_4N_2O_2^+$  and the fragments  $CNO$ ,  $C_3H_3NO^+$ ,  $C_3H_2NO^+$ , and  $C_4H_4O^+$ . Moreover, the scheme of the uracil fragmentation also predicts the formation of neutral fragments, which can also be in excited states (the dissociative excitation). First of all, these are the fragments  $CO$  (at the decay of ion  $C_3H_3NO^+$ ),  $HNCO$  and  $C_3H_3NO$  (at the decay of molecular ion  $C_4H_4N_2O_2^+$ ), and  $H$  (at the decay of ion  $CHNO^+$ ). The radiative decay of the excited states of charged and neutral fragments should somehow manifest itself in the emission spectrum of uracil.

For instance, the band with a maximum at the wavelength  $\lambda = 205.5$  nm is evidently a superposition of a few emission lines belonging to the ion  $CO^+$  (the first negative system, the electron transition  $B^2\Sigma^+ \rightarrow X^2\Sigma^+$ ,  $\lambda_M = 206.8, 206.1, \text{ and } 204.2$  nm). The band with a maximum at  $\lambda = 218.5$  nm is a superposition of several emission lines belonging to a molecule  $CO$  (the fourth positive system, the transition  $A^1\Pi \rightarrow X^1\Sigma^+$ ,  $\lambda = 217$  nm) and the ion  $CO^+$  (the first negative system, the electron transition  $B^2\Sigma^+ \rightarrow X^2\Sigma^+$ ,  $\lambda = 219$  nm). The band with a maximum at  $\lambda = 241.9$  nm belongs to an ion  $CO^+$  (the first negative system, the electron transition  $B^2\Sigma^+ \rightarrow X^2\Sigma^+$ ,  $\lambda = 241.9$  nm). In the bands with maxima at the wavelengths  $\lambda = 256.4$  and  $297.2$  nm, there are lines given by the neutral fragment  $CO$  (the third positive system, the transition  $A^1\Pi \rightarrow X^1\Sigma^+$ ,  $\lambda = 256.2$  and  $297.3$  nm). The band with a maximum at

$\lambda = 265.3$  nm is obviously a superposition of two emission lines of the ion  $CO^+$  (the first negative system, the electron transition  $B^2\Sigma^+ \rightarrow X^2\Sigma^+$ ,  $\lambda_M = 267.2$  and  $263.9$  nm).

A separate attention should be paid to the most intensive band in the spectrum with a maximum at the wavelength  $\lambda = 275$  nm. In our opinion, its appearance is connected with the radiative decay of the first excited electron-vibrational state of an uracil molecular ion into the ground state. The following speculations confirm this hypothesis. First, as Table 1 demonstrates, the cross-section of formation of the molecular ion is the largest. Hence, it is reasonable to expect that the cross-sections of formation of the molecular ion in the excited states – the lowest ones in the first place – should also be larger than those for other charged fragments in excited states. This factor can explain the largest spectral intensity of the band with a maximum at the wavelength  $\lambda = 275$  nm. Second, the intense peak at an energy of about 14 eV was found in the photoelectric spectrum obtained at the uracil photoionization, which was presented in work [25]. If we sum up the energy of spectral transition (at  $\lambda = 275$  nm) and the energy of uracil ionization ( $9.4 \pm 0.2$  eV), we obtain a value of about 13.9 eV, which practically coincides with the energy position of the peak in the photoelectric spectrum. Therefore, we may suppose that the molecular ion of uracil has an excited electron-vibrational state at an energy of about 13.9 eV, from which the radiative transition into the ground state of ion is possible.

As one can see from Fig. 6, in the wavelength interval 300–440 nm, two wide molecular bands are observed, which partially overlap each other and serve a pedestal (a background) for other narrower bands. We identify one of them with the radiation emission of an uracil molecule in a singlet state, and the other with that of the same molecule in a triplet state. This interpretation does not contradict the results of our calculations, which were executed with the use of the AM1 semiempirical method with the help of the HyperChem 8.0 software package. Note that, when films of polycrystalline uracil are photoexcited, two maxima located at wavelengths of about 350 and 420 nm emerge in its broad luminescence band [20, 21].

The spectral band at  $\lambda = 317.1$  nm (see Fig. 6) can be emitted by the pyrimidine ring (transitions A–X). The band at  $\lambda = 328.4$  nm is made up of radiation emission contributions by the fragments  $CN^+$  (transitions  $C^1\Sigma - A^1\Sigma$ ) and  $NCN$  (transitions  $^3\Pi_u - ^3\Sigma_g$ ). The band with a maximum at  $\lambda = 333.5$  nm is emitted by the  $NCN$  group (transition  $^3\Pi_u - ^3\Sigma_g$ ), and the bands

**Table 3.** Cross-sections of the formation of positive ions of uracil molecules at an electron energy of 95 eV (in terms of  $10^{-16}$  cm<sup>2</sup> units)

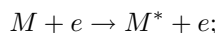
$m/z$	Ions	This work	[13] Measurements
112	$C_4H_4N_2O_2^+$	2.7	4.5
69	$C_3H_3N_O^+$	1.1	2.3
42	$CNO^+C_2H_2O^+; CH_2N_2^+$	1.0	2.0

with maxima at  $\lambda = 344.5$  and  $357.3$  nm correspond to the HNCN group (transitions A-X). The neutral fragment CO of comet ( $379.6$  nm) and Herzberg ( $389.3$  nm) systems reveals itself by emitting at  $\lambda = 377.1$  and  $388.3$  nm. The band at  $\lambda = 411.5$  nm is formed by the fragments CO (transitions in the Herzberg system,  $412.5$  nm) and hydrogens ( $H_\delta$ ,  $410.1$  nm). The intense line at  $\lambda = 421.0$  nm belongs to the fragment  $CH^+$  (transition A-X,  $\lambda = 421.0$  nm). The radiation emission by the neutral fragment CO reveals itself in the band at a wavelength of  $427.3$  nm (the comet system,  $\lambda = 427.3$  nm) and the band at  $451.1$  nm (the Angström system,  $\lambda = 451.0$  nm). The excitation of the CO and  $CO^+$  bands mentioned above by means of the electron impact was studied in work [25] in detail. Some spectral bands may contain a contribution from hydrogens (the Balmer series). In particular, these bands have maxima at  $\lambda = 398.4$  nm ( $H_\epsilon = 397.07$  nm),  $\lambda = 412.3$  nm ( $H_\delta = 410.1$  nm), and  $\lambda = 427.3$  nm ( $H_\gamma = 434.05$  nm). The hydrogen line  $H_\beta$  at  $\lambda = 486.1$  nm is observed especially distinctly.

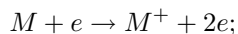
#### 4. Discussion of Results

First of all, we would like to note that the results to be discussed were obtained by us for a molecular object that has an exclusive biological importance. Uracil, together with other nitrogenous bases – thymine, adenine, cytosine, and guanine – is an important component of genetic macromolecules, nucleic acids.

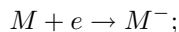
Schematically, the set of basic physical processes with the participation of a molecule  $M$  in inelastic interactions with an electron  $e$  can be classed as follows: molecular excitation,



formation of a positive molecular ion,



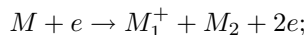
formation of a negative molecular ion



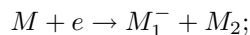
dissociative excitation,



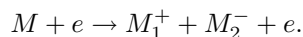
dissociation with the formation of a positive ion,



dissociative ionization with the formation of a negative ion,



and dipolar dissociation,



Other transformations are also possible. For instance, in addition to excited and ionized products, neutral fragments can also be formed, which are rather difficult to be identified. Note that the processes given above run practically simultaneously at high rates and with different probabilities. Therefore, for the explanation of specific experimental results to be adequate, the contributions of various channels have to be taken into account.

We should also bear in mind that, owing to inelastic interactions between slow electrons and molecules and in contrast to photo-induced processes, the direct excitation of metastable triplet states becomes possible. We may suppose that it is through such long-living excited states that the conditions for the resonance formation of negative ions are created. The direct formation of the triplet excited states of cytosine and thymine molecules was shown in our previous works (see, e.g., works [2] and [7], respectively). For the interpretation of data obtained for uracil to be more complete, it is expedient to experimentally study the excitation functions of corresponding spectral bands and their energy thresholds. We are planning to fulfill those tasks in our future researches.

The issue concerning the role of negative ions in biostructures remains open. The resonance nature of the formation of negative ions at low (just this circumstance is very essential!) energies gives ground to assume that the given mechanism is responsible for considerable damages in macromolecules of nucleic acids. According to our estimates, the formation cross-section for uracil negative ions is approximately 500 times as small as the corresponding cross-section for positive ions. However, this fact is not sufficient to be a basis for the conclusion that the resulting destructive influence of negative ions is less than that of positive ions, because their reactivities are different. Moreover, one should bear in mind that the probability for a whole negatively ionized molecule to appear and get stabilized becomes larger if the concentration of particles is high, e.g., under the conditions in a living cell.

It is also important that, as follows from relation (1), the low-energy electrons produce atomic hydrogen – besides negative ions of uracil and its complicated fragments – in the cell. The initial localizations of hydrogen atoms are unknown. However, is not excluded that

the hydrogens can be detached from atoms C5 and C6 in the pyrimidine ring. Generally speaking, this scenario is possible, because, as the results of our calculations show, the regions of large positive charge are concentrated here. Therefore, these regions are the most probable places for the first electron attack.

Concerning the uracil excitation with slow electrons, the emission spectrum of uracil initiated by an electron impact in this energy range is governed by various processes. First, these are the spectral transitions between electron-vibrational-rotational states of both the whole uracil molecule and the molecular ion. For such a multiatomic molecule, the most probable transitions are only those from the lowest singlet and triplet electron states into the ground state. The same is valid for the molecular ion. Second, these are also the spectral transitions between electron-vibrational-rotational states of molecule fragments that were formed under the action of an electron impact (the processes of dissociative excitation and dissociative ionization with excitation).

At last, it is very important to understand that the ionization, fragmentation, and excitation of molecules of nucleotide bases induce changes in the primary and secondary structures of important bioinformative macromolecules (RNA and DNA) even if the electron energy is low. First of all, we should expect a destabilization in the system of hydrogen bonds between complementary base pairs, a degradation of nucleotides, and genotoxic modifications. As a result, the irreversible degradation and mutagenic processes can be initiated in living cells even at insignificant influence energies.

## 5. Conclusions

The processes of ionization and excitation of isolated uracil molecules at their collisions with low-energy electrons have been studied. The data on the formation cross-sections have been obtained for negative and positive ions of uracil, the nitrogenous base of nucleic acids. It was shown that the formation cross-section of negative ions reaches its maximum value at an energy of bombarding electrons of 1.1 eV, with the magnitude being equal to  $5.0 \times 10^{-18} \text{ cm}^{-2}$ . The absolute value and the energy dependence of the formation cross-section were also determined for the positive ions for uracil in the range of electron energies from the threshold ( $9.4 \pm 0.2 \text{ eV}$ ) to 200 eV. The maximum of the ionization cross-section is attained at an energy of 95 eV and is equal to  $(1.0 \pm 0.1) \times 10^{-15} \text{ cm}^{-2}$ . It was experimentally found that the electrons with energies of a few electronvolts (below the threshold energies of elec-

tron excitation and positive ionization) effectively destroy the uracil molecule, producing a mobile hydrogen radical and a negatively charged fragment of uracil.

The interaction of slow electrons with uracil molecules in the gas state is accompanied by the emergence of a complicated emission spectrum in the range 200–490 nm, which testifies to an intense fragmentation of molecules. The radiation spectrum of uracil is formed by the processes of dissociative excitation of molecules, dissociative excitation with ionization, and excitation of electron levels in both the initial molecule and the molecular ion. The data obtained can be used to estimate radiation-induced changes in DNA and RNA molecules at the internal  $\beta$ -irradiation of bioobjects.

1. M.I. Sukhoviya and I.I. Shafranyosh, in *Mechanisms of Radiation-Induced Damage and Recovery of Nucleic Acids* (Pushchino Sci. Center of the RAS, Pushchino-na-Oke, 1980), p. 51 (in Russian).
2. M.I. Sukhoviya, V.N. Slavik, I.I. Shafranyosh, and L.L. Shimon, *Biopolim. Klet.* **7**, 77 (1991).
3. M.I. Sukhoviya, M.I. Shafranyosh, and I.I. Shafranyosh, in *Spectroscopy of Biological Molecules: New Directions* (Kluwer, Dordrecht, 1999), p. 281.
4. V. Cobut, Y. Frongillo, J.P. Patau, T. Goulet, M.J. Fraser, and J.P. Jay-Gerin, *Radiat. Phys. Chem.* **51**, 229 (1998).
5. I.I. Shafranyosh, M.I. Sukhoviya, and M.I. Shafranyosh, *J. Phys. B* **39**, 4155 (2006).
6. I.I. Shafranyosh, M.I. Sukhoviya, M.I. Shafranyosh, and L.L. Shimon, *Zh. Tekhn. Fiz.* **78**, N 12, 7 (2008).
7. I.I. Shafranyosh and M.I. Sukhoviya, *Opt. Spektrosk.* **102**, 553 (2007).
8. L.V. Gurvich, G.V. Karachevtsev, V.N. Kondrat'ev, Yu.A. Lebedev, V.A. Medvedev, V.K. Potapov, and Yu.S. Khoddev, *Energies of Chemical Bond Breaking. Ionization Potentials and Electron Affinity* (Nauka, Moscow, 1974) (in Russian).
9. G. Hanel, B. Gstir, S. Denifl *et al.*, *Phys. Rev. Lett.* **90**, 188104 (2003).
10. S. Steenken, J.P. Telo, H.M. Novais, and L.P. Candeias, *J. Am. Chem. Soc.* **114**, 4701 (1992).
11. R.A. Khmel'nitskii and B.P. Terent'ev, *Usp. Khim.* **48**, 854 (1979).
12. A.A. Polyakova, *Molecular Mass Spectrometric Analysis of Organic Compounds* (Khimiya, Moscow, 1973) (in Russian).
13. S. Feil, K. Gluch, S. Matt-Leuber, P. Scheier, J. Limtrakul, M. Probst, H. Deutsh, K. Becker, A. Stamatovic, and T.D. Mark, *J. Phys. B* **37**, 3013 (2004).

14. NIST Standard Reference Database. Webpage 14. [http://webbook.nist.gov/chemistry]; AIST Spectral Database for Organic Compounds [http://riodb01.ibase.aist.go.jp/sdbs/cgi-bin/direct\_frame\_top.cgi]
15. M.I. Shafranyosh, *Nauk. Visnyk Uzhgorod. Univ. Ser. Fiz.* **25**, 208 (2009).
16. H. Deutsch, K. Becker, S. Matt, and T.D. Mark, *Plasma Phys. Control. Fusion* **40**, 1721 (1998).
17. H. Deutsch, P. Scheier, S. Matt-Leubner, K. Becker, and T.D. Mark, *Int. J. Mass Spectr.* **243**, 215 (2005).
18. H.A. Bethe, *Intermediate Quantum Mechanics* (Benjamin, New York, 1964).
19. N.F. Mott and H.S.W. Massey, *The Theory of Atomic Collisions* (Oxford Univ. Press, Oxford, 1965).
20. I.P. Vinogradov, V.V. Zemskikh, and N.Ya. Dodonova, *Opt. Spektrosk.* **36**, 596 (1974).
21. K.P. Huber and G. Herzberg, *Molecular Spectra and Molecular Structure IV: Constants of Diatomic Molecules* (Van Nostrand, New York, 1979).
22. G. Herzberg, *Molecular Spectra and Molecular Structure I: Spectra of Diatomic Molecules* (Van Nostrand, New York, 1950).
23. R.W. Pearse and A.G. Gaydon, *The Identification of Molecular Spectra* (Chapman and Hall, London, 1976).
24. V.V. Skubenich, M.M. Povch, and I.P. Zapesochnyi, in *Abstracts of the 7th All-Union Conference on Physics of Electron and Atomic Collisions* (Petrozavodsk, 1978), Pt. 1, p. 102.
25. H-W. Johims, M. Schwel, H. Baumgartel, and S. Leach, *Chem. Phys.* **215**, 263 (2005).

Received 26.11.11.

Translated from Ukrainian by O.I. Voitenko

#### ІОНІЗАЦІЯ ТА ЗБУДЖЕННЯ МОЛЕКУЛ УРАЦИЛУ ЕЛЕКТРОННИМ УДАРОМ

*М.І. Суховія, М.І. Шафраньош, М.М. Чаварга, І.І. Шафраньош*

#### Резюме

Експериментальним шляхом отримано дані про абсолютні величини перерізів утворення позитивних і негативних іонів азотистої основи нуклеїнових кислот – урацилу. Показано, що максимальних значень переріз утворення негативних іонів досягає при енергії бомбардуючих електронів 1,1 еВ, і його абсолютна величина становить  $5,0 \cdot 10^{-18}$  см<sup>2</sup>. Визначено абсолютну величину та енергетичну залежність перерізу утворення позитивних іонів для урацилу в інтервалі енергій електронів від порога до 200 еВ. Максимум перерізу іонізації знаходиться при енергії 95 еВ і дорівнює  $(1,0 \pm 0,1) \cdot 10^{-15}$  см<sup>2</sup>. Отримано спектри люмінесценції ізольованих молекул урацилу в області довжин хвиль 200–500 нм під дією повільних електронів. У спектрі спостерігаються близько 20 спектральних смуг і ліній. Показано, що спектр випромінювання урацилу формують процеси дисоціативного збудження молекул, дисоціативного збудження з іонізацією, збудження електронних рівнів вихідної молекули та молекулярного іона. Обговорено біофізичні наслідки отриманих результатів.